DMD Fast Forward. Published on February 12, 2007 as doi:10.1124/dmd.106.013474

Differential subcellular distribution of mitoxantrone in relation to chemosensitization in two human breast cancer cell lines

Sophie VIBET, Karine MAHEO, Jacques GORE, Pierre DUBOIS, Philippe BOUGNOUX and Igor CHOURPA*

SV, KM, JG, PB - *INSERM, E 0211, "Nutrition, Croissance et Cancer", Tours, F-37000 France; Université François-Rabelais, Tours, F-37000 France ; IFR 135 "Imagerie Fonctionnelle", Tours, F-37000 France.*

IC, PD - *Université François-Rabelais, Faculté de Pharmacie, "Focalisation magnétique d'agents anticancéreux", Tours, F-37200 France; IFR 135 "Imagerie Fonctionnelle", Tours, F-37000 France.*

*- corresponding author

Running title: Subcellular distribution of mitoxantrone and chemosensitization

Corresponding author :

Professor Igor CHOURPA,
Faculté de Pharmacie,
31 avenue Monge
37100 Tours, France.
Tel: 33-247367162 ;
Fax : 33-247367270.
e-mail : chourpa@univ-tours.fr

Number of text pages: 28

Number of tables: 1

Number of figures: 5

Number of references: 37

Number of words in the *Abstract:* 250

Introduction: 696

Discussion: 898

Nonstandard abbreviations used in the paper:

CSI - confocal spectral imaging

DHA - docosahexaenoic acid

MTX - mitoxantrone

NAC - N-acetyl-L-cysteine

ROS – reactive oxygen species

DMD Fast Forward. Published on February 12, 2007 as DOI: 10.1124/dmd.106.013474
This article has not been copyedited and formatted. The final version may differ from this version.

ABSTRACT

The present work investigates the relation between cancer cell chemosensitivity and subcellular distribution, molecular interaction and metabolism of an anticancer drug. To get insights into this relation, we took advantage of the differential sensitivity of two breast cancer cell lines, MDA-MB-231 and MCF-7 to anthracyclins, along with the property of docosahexaenoic acid (DHA, 22:6n-3), to differentially enhance their cytotoxic activity. The fluorescent drug mitoxantrone (MTX) was utilized because of the possibility to study its subcellular accumulation by confocal spectral imaging (CSI). CSI allowed us to obtain semi-quantitative maps of four intracellular species: nuclear MTX bound to DNA, MTX oxidative metabolite in endoplasmic reticulum, cytosolic MTX and finally, MTX in a low polarity environment characteristic of membranes. MDA-MB-231 were found to be more sensitive to MTX (IC_{50} = 18 nM) than MCF-7 (IC_{50} =196 nM). According to fluorescence levels, the nuclear and cytosolic MTX content was higher in MCF-7 than in MDA-MB-231, indicating that mechanisms other than nuclear MTX accumulation account for chemosensitivity. In the cytosol, the relative proportion of oxidized MTX was higher in MDA-MB-231 (60%) than in MCF-7 (7%). DHA sensitized MDA-MB-231 (about 4 fold) but not MCF-7 cells to MTX and increased MTX accumulation by 1.5 fold in MDA-MB-231 only. The DHA-stimulated accumulation of MTX was mainly attributed to the oxidative metabolite. Antioxydant N-acetyl-L-cystein inhibited the DHA effect on both metabolite accumulation and cell sensitization to MTX. We conclude that drug metabolism and compartimentalization are associated with cell chemosensitization and the related cytotoxicity mechanisms may involve oxidative stress.

Experimental studies have shown that exogenous n-3 polyunsaturated fatty acids (PUFAs) may sensitize tumor cells to anticancer drugs, in cell culture or in animal tumors (Shao et al., 1995; Germain et al., 1999; Colas et al., 2004; Menendez et al., 2004; Menendez et al., 2005). These effects of n-3 PUFA have been found to be inhibited by the presence of antioxidants (Germain et al., 1998; Colas et al., 2004; Colas et al., 2005; Menendez et al., 2005). Several mechanisms have been proposed to account for the effect of PUFAs in increasing anti-cancer drug efficacy. These include increase in drug transport across cell membrane (Burns and North, 1986; Spector and Burns, 1987), generation of free oxygen radicals and lipid peroxidation (Das, 1999; Rose and Connolly, 1999; Stoll, 2002). Among PUFAs, docosahexaenoic acid (DHA, a long chain omega-3 polyunsaturated fatty acid) was the most potent to enhance the cytotoxic effect of doxorubicin in MDA-MB-231 breast cancer cell line (Germain et al., 1999). Recently, we found that the DHA-induced increase in doxorubicin cytotoxicity was cell line-dependent and linked to oxidative stress (Maheo et al., 2005).

Mitoxantrone (MTX), an anthracenedione, has a spectrum of clinical activity similar to that of anthracyclines. Antineoplastic activity of anthracyclins and anthracenediones has been mainly attributed to topoisomerase II inhibition and to reactive oxygen species (ROS) production (Gewirtz, 1999). However MTX has been shown to generate free radicals to a much lesser degree than doxorubicin (Novak and Kharasch, 1985). Little is known about the effect of DHA on chemosensitivity of breast cancer cell lines to MTX. Supplementation of leukemia cells by DHA led to an increase in MTX uptake (Burns et al., 1988a) but no change in intracellular distribution of the drug was detected in subcellular fractions obtained by differential centrifugation and sucrose gradient separation after cellular disruption (Burns et al., 1988b).

A direct way to study the intracellular accumulation of fluorescent MTX (Bell, 1988) consists in use of flow cytometry and fluorescence microscopy. High-resolution images of MTX intracellular distribution in various cell lines have been obtained with confocal fluorescence microscopy (Smith et al., 1992; Fox and Smith, 1995; Consoli et al., 1997; Kellner et al., 1997; Smith et al., 1997; Hazlehurst et al., 1999; Litman et al., 2000). Nevertheless, band-pass analysis of the fluorescence intensity in confocal fluorescence microscopy limited the analysis to the overall drug detection and did not account for the fluorescence changes depending on the drug environment/interaction.

In alternative to confocal fluorescence microscopy, confocal spectral imaging (CSI) technique is based on measurement, at different points of a cell, of the fluorescence spectra, allowing to distinguish different molecular states of intracellular drug (Sharonov et al., 1994). CSI has been recognized as a potent tool for direct qualitative and quantitative study of MTX within compartments of living K562 cells (Feofanov et al., 1997a; Feofanov et al., 1997b; Feofanov et al., 1999). The main limitation of these CSI studies was a low sensitivity related to the use of the green light (514.5 nm) for excitation of red-absorbing MTX. As a consequence, the MTX concentrations used by Feofanov et al. during cells treatment had to be very high: 5-10 μM.

We have performed a CSI scanning of MTX-treated MCF-7 and MDA-MB-231 cells by using resonance excitation with a red laser line (632.8 nm). Compared to previously published CSI method (Feofanov et al., 1997a; Feofanov et al., 1997b; Feofanov et al., 1999), increased selectivity and sensitivity of intracellular MTX detection were achieved. The present CSI study better respects cellular physiology, through a reduction of cell exposure to both drug concentration (0.5 μM) and laser radiation (30 μW and 0.02 s per spectrum). Four intracellular species of MTX were thus identified and a particular attention was paid to characterize the fluorescence of an oxidative metabolite of the drug.

We compared the intracellular distribution of the molecular species of MTX within two breast cancer cell lines, MCF-7 and MDA-MB-231, and examined the influence of DHA supplementation on this distribution. Our aim was to take advantage of the differential sensitivity of these two breast cancer cell lines to MTX and DHA in order to get insights into the mechanisms responsible for chemosensitization.

METHODS

Drugs and chemicals. Unless otherwise stated, all chemicals were purchased from Sigma (Sigma-Aldrich Chimie, France). Dilutions of mitoxantrone (Novantrone®, 10 mg/5ml, Wyeth Lerderle) were freshly prepared in Dulbecco's modified Eagle's medium (DMEM) containing 5% heat-inactivated fetal calf serum, 50 UI/ml penicillin and 50 µg/ml streptomycin (Cambrex, France). N-acetyl-L-cysteine (NAC) was used at 10 mM in DMEM medium. Docosahexaenoic acid (DHA, 22:6n-3) methyl ester was used for this study. The fatty acid was dissolved in 99% ethanol and stored as stock solution (150 mM) under nitrogen at -80° C. For all experiments, fatty acid was prepared freshly from stock solution and diluted with growth culture medium (final ethanol concentration: 0.02%). ER-Tracker™ Green, rhodamine 123 and CM-H_2DCFDA (5-(and-6)-chloromethyl-2',7'-dichlorodihydrofluorescein diacetate) were purchased from Molecular Probes (Invitrogen, France).

Cell culture. The human breast carcinoma cell lines MDA-MB-231 and MCF-7 were obtained from American Type Culture Collection (LGC Promochem, France). Cell lines were cultured in Dulbecco's modified Eagle's medium (DMEM) containing 5% heat-inactivated fetal calf serum, 50 UI/ml penicillin and 50 µg/ml streptomycin (Cambrex, France). Cells were cultured at 37° C in a humidified incubator with 5% CO_2. The culture medium was changed each 24 h.

Drug cytotoxicity. Cells were seeded in standard 96-well plates (7 x 10^3 cells/well). One day after seeding, the culture medium was changed and replaced by medium containing different concentration of MTX (MTX: 10^{-5} to 5 µM) with or without DHA (30 µM) during 7 days. Viability of cells were measured as a whole by the tetrazolium salt assay (Mosmann, 1983).

Cells were incubated at 37°C for 1 hour with the tetrazolium salt (3-[4,5-dimethylthiazol-2-yl]-2,5-diphenyl tetrazolium bromide) and metabolically active cells reduced the dye to purple formazan. Formazan crystals were dissolved with DMSO. Absorbance was measured at 570 nm using a multi-well plate reader (Molecular Devices, SpectraMax 190 model). Dose response curves were plotted as percentages of the control cell absorbance which was obtained from control wells (without MTX treatment). These values were fitted to sigmoidal dose-response model (GraphPad Prism®, GraphPad Software Inc):

$$Y = Min + (Max - Min) / (1 + 10^{Log\ IC_{50} - X})$$

with :

Y = viability (in %)

X = Log (MTX concentration, in µM)

Min = minimum viability

Max = maximum viability

IC_{50} = concentration of MTX producing a 50% decrease of viability

Instrumental setup for confocal multispectral imaging (CSI). Fluorescence measurements were carried out using a LabRam confocal microspectrometer (Horiba-Jobin Yvon, France) equipped with a low dispersion grating (300 grooves per mm) and with an automated X-Y-Z scanning stage. A colour camera (Panasonic, WV-CP454E) together with a VITEC video card provided a digitalized TV image of a sample illuminated with a white light source (phase-contrast optical view).

MTX fluorescence was excited with a 632.8 nm line of an internal, air-cooled, helium-neon laser. The power on the samples was ≈ 30 µW, the acquisition time was 0.02 s or 0.05 s per spectrum. Particular attention was paid to normalize the measured signal on acquisition time as well as on instrumental response, using a Si-plate and a fluorescein solution as

DMD Fast Forward. Published on February 12, 2007 as DOI: 10.1124/dmd.106.013474
This article has not been copyedited and formatted. The final version may differ from this version.

intensity standard. Sample irradiation and collection of fluorescence were performed through a 100× microscope objective (numerical aperture 0.90; Olympus, Japan). The confocal hole aperture was adjusted to 100 µm to obtain ca. 0.8 µm lateral and ca. 3.5 µm axial resolution. The spectral resolution was 1 nm.

Performing CSI mapping on living cells. The breast cancer cells (treated with or without DHA during 7 days) were incubated with MTX (0.5 µM) for 1 hour at 37°C, 5% CO_2. When N-acetyl-L-cysteine (NAC, 10 mM) was used, a preincubation (15 min) of the cells with NAC was performed before the incubation with MTX. Before CSI analysis, the medium containing drug was removed and the cells were resuspended in fresh medium after two rinses with fresh medium (pH 7.4). A drop of this preparation was put on a microscope glass slide and covered with a thin cover-slide. Isolated cells, selected for the apparently intact morphology, were analyzed individually.

To study the subcellular repartition of MTX, we used the 2D mapping of an optical section at half-thickness of the cell. Cells were scanned within X-Y plane with fixed step of 0.8 µm that provided maps containing typically ca. 900 spectra (30×30 points). The acquisition time was less than 2-3 min per entire cell map. Both acquisition and treatment of multispectral maps were performed with LabSpec software.

Generating chemical maps from spectral sets. Subcellular drug repartition was studied via analysis of both intensity and shape of fluorescence spectra within CSI maps, as described previously (Sharonov et al., 1994; Feofanov et al., 1997b). Briefly, each experimental spectrum recorded in a confocal mode from a cell was fitted to a sum of four reference spectra of MTX taken with appropriate coefficients:

$$F_{Total}(\lambda) = C_{DNA}F_{DNA}(\lambda) + C_{cyt}F_{cyt}(\lambda) + C_{met}F_{met}(\lambda) + C_{lp}F_{lp}(\lambda)$$

where F_{DNA}, F_{cyt}, F_{met} and F_{lp} are the fluorescence spectra of respectively MTX-DNA complex, cytosolic complex of native MTX, cytosolic complex of metabolized MTX and MTX in low polarity environment, referred to a unitary intensity (Figure 1). Each of these MTX species has a characteristic fluorescence spectral shape established by *in vitro* modeling. The values of C_{DNA}, C_{cyt}, C_{lp} and C_{met} are spectral contribution factors of the respective drug species. These factors could be converted into concentrations, once the fluorescence yield of each of the above fluorophores will be known.

The fitting results were optimized with least square method. The fitting error was below 5 % (typically 2-3 %). The cellular autofluorescence was completely neglected, because of the absence of any significant fluorescence of the untreated cells under the conditions used.

The spectral contribution factors of each MTX species were used to generate the respective 2D distribution map (thereafter referred to as a chemical map) over the cell. In this manner, four model-specific chemical maps were generated for each cell.

In view of significant cell-to-cell variations of the fluorescence intensity, each chemical map was brought to a relative intensity scale by normalizing all the spectra on the intensity of the most intense spectrum (typically that from nucleoli). Thus, the chemical maps reflected qualitatively the repartition of the drug within subcellular compartments.

Quantification of MTX cellular accumulation and distribution. Two kinds of quantitative information were extracted from analysis of each map- average spectrum: (i) First of all, fluorescence intensity (expressed in arbitrary units, thereafter called fluorescence level) in the spectral region between 645 and 935 nm was considered as representative of overall intracellular MTX accumulation, (ii) Then, the average spectrum was fitted to a sum of four reference MTX spectra described above. The obtained contribution factors were interpreted as

DMD Fast Forward. Published on February 12, 2007 as DOI: 10.1124/dmd.106.013474
This article has not been copyedited and formatted. The final version may differ from this version.

cell-average relative contents (fluorescence levels) of the specific drug species. The results were averaged over 16 to 23 cells for each kind of treatment.

Co-localization of MTX oxidative metabolite with cellular organelles. We labelled endoplasmic reticulum and mitochondria using two organelle-specific fluorophores, ER-Tracker™ Green and rhodamine 123, respectively. MDA-MB-231 cells, treated for 1 hour with 0.5 µM MTX and washed in PBS, were incubated for 20 minutes with 0.5 µM ER-Tracker™ Green or 1 µM rhodamine 123. Co-localization studies were performed using a 488 nm line of an Ar^+ laser. The estimated laser power at the sample was ~20 µW. The fluorescence spectra were recorded with acquisition time of 1 sec per spectrum. The CSI spectral maps were generated as described above.

Measurement of reactive oxygen species (ROS). Cells were cultured in 9 cm^2 multiwell plates and treated with MTX at IC_{50} during 7 days. Cells were washed twice with Hanks-Hepes solution (pH 7.3, 37°C) and then incubated during 30 min with 10 µM CM-H_2DCFDA, in the dark at 37°C. CM-H_2DCFDA is an indicator for reactive oxygen species (hydrogen peroxide, hydroxy and peroxyl radicals). Then, cells were washed twice with cold Hanks-Hepes (pH 7.3, 4°C) solution, and sonicated in 1 mL of distilled water (4°C). Whole cells lysates were centrifuged (10 000 x g, 5 min, 4°C) and fluorescence intensities were measured on supernatants at 522 nm (excitation wavelength: 480 nm) with a Hitachi F-2500 spectrofluorimeter. For each supernatant, protein concentration was measured with BCA kit (Uptima®, Interchim, France) and the normalized fluorescence (arbitrary units of fluorescence / mg proteins) was calculated.

Statistics. Statistical analysis was carried out using Student's unpaired t-test, one-way ANOVA and Newman-Keuls multiple comparison tests (GraphPad Prism®, GraphPad Software Inc); $p < 0.05$ was regarded as significant.

DMD Fast Forward. Published on February 12, 2007 as DOI: 10.1124/dmd.106.013474
This article has not been copyedited and formatted. The final version may differ from this version.

RESULTS

MTX cytotoxicity. Breast cancer cells were cultured for 7 days in a medium supplemented with MTX concentrations ranging from 10^{-5} µM to 5 µM, without (control) or with 30 µM DHA. DHA 30 µM was not toxic (trypan blue exclusion, data not shown).

In control conditions (absence of DHA), concentrations of MTX inducing 50% cell mortality (IC_{50}) were different in the two cell lines (18 ± 6 nM for MDA-MB-231 and 196 ± 70 nM for MCF-7). Figure 2 shows the corresponding dose-response curves. Supplementation of MCF-7 cells with DHA did not modify significantly MTX cytotoxicity : IC_{50} = 128 ± 74 nM *versus* 196 ± 70 nM in supplemented *versus* no supplemented cells, respectively ($p > 0.05$). In contrast, in MDA-MB-231 cells, DHA supplementation led to an increase in MTX toxicity at concentration comprised between 10^{-1} and 10^{-3} µM: IC_{50} shifted from 18 ± 6 nM to 4 ± 1 nM. This 4.5-fold enhancement of MTX cytotoxicity by DHA was statistically significant ($p < 0.001$). Cell viability experiments were also performed in presence of the antioxidant N-acetyl-L-cysteine (NAC). Control or DHA-supplemented MDA-MB-231 cells were treated with MTX at several concentrations ranging from 10 to 40 nM in presence of NAC. Addition of NAC (10 µM for 7 days) suppressed the enhancing effect of DHA on cell sensitivity to MTX, since cell viability remained unchanged between control and DHA-supplemented cells upon treatment with MTX.

DMD Fast Forward. Published on February 12, 2007 as DOI: 10.1124/dmd.106.013474
This article has not been copyedited and formatted. The final version may differ from this version.

Overall accumulation and chemicals maps of MTX subcellular distribution. The results on overall drug accumulation in the two cell lines are presented in Table 1. In control conditions, the overall drug fluorescence level in MDA-MB-231 was 2.5-fold lower than in MCF-7. DHA supplementation led to a 1.5-fold increase in overall MTX accumulation ($p < 0.001$) in MDA-MB-231, while no significant change was observed in MCF-7.

At a single-cell level, the most intense fluorescence was found in nucleoli (intensity of 100 %) and in nucleus (intensity of 50-70 %). The intensity observed in cytosol was between 20 and 40 %. It was about 10 % in cell periphery (membrane).

Due to the possibility of spectral analysis of intracellular fluorescence inherent to the CSI approach, four specific maps characteristic of molecular environment/species of MTX were generated in each cell (Figure 3A). The maps of MTX-DNA fluorescence had nuclear localization. DHA treatment did not induce any change in these maps. Fluorescence of the MTX-metabolite had typically a strong perinuclear spot and a weaker diffusion within the cytosol. The metabolite maps were larger and more intense in MDA-MB-231 than in MCF-7. DHA supplementation resulted in a strong increase of the metabolite fluorescence in both cell lines. In contrast, this increase was inhibited in the cells treated with NAC antioxydant. The cytosolic complex of native MTX was distributed all over the cytosol. This staining was different in the two cell lines: homogeneous in MCF-7 and with multiple spots distribution in MDA-MB-231. Supplementation with DHA led to a decrease in level of native MTX cytosolic complex, particularly in MDA-MB-231. Maps of MTX in low polarity environment fitted cellular contours (plasmic membranes) as well as several perinuclear spots (intracellular membranes). After DHA supplementation, this staining was reduced, mainly in intracellular membranes.

DMD Fast Forward. Published on February 12, 2007 as DOI: 10.1124/dmd.106.013474
This article has not been copyedited and formatted. The final version may differ from this version.

Co-localization of specific species of MTX. Deconvolutions of spectra from nuclear region corresponded to a 100 % contribution of characteristic fluorescence assigned to MTX-DNA complexes. In contrast to the nuclear fluorescence, the spectra from other cellular regions were decomposed into variable contributions of two or three reference spectra, thus indicating co-localization of corresponding molecular species of MTX (Figure 3B). Spectra from the intense perinuclear regions were particularly mixed, since they corresponded to the spectrum of the cytosolic complex of native MTX enriched with the fluorescence of the complex of the metabolized MTX and complemented with the spectrum characteristic of MTX in low polarity environment (intracellular membranes). This is illustrated by certain similarity of the respective maps seen in Figure 3A, all having bright spots in the perinuclear regions. The co-localization was confirmed after superposition of the respective maps encoded in pseudo-colors (Figure 3B): the white perinuclear spots correspond to a mixture of three colours, i.e. of three species, indicating that the cytosolic complex of metabolized MTX is located in perinuclear regions enriched with membranes.

To check a possible assignment of these regions to cellular organelles such as mitochondria or endoplasmic reticulum, we stained the MDA-MB-231 cells with rhodamine 123 and ER-Tracker™ Green, respectively. The excitation wavelength of 488 nm was used, because it was optimum for ER-Tracker™ Green and rhodamine 123 (emission maxima at 517 and 540 nm, respectively) and was still suitable to detect the MTX metabolite. According to the CSI data, the metabolite fluorescence was co-localized with fluorescence of ER-Tracker™ Green (Fig. 4) but not with fluorescence of rhodamine 123 (data not shown).

Cell-average intracellular content of the specific species of MTX. Average fluorescence levels corresponding to the four specific species of MTX are shown in Fig. 5.

DMD Fast Forward. Published on February 12, 2007 as DOI: 10.1124/dmd.106.013474
This article has not been copyedited and formatted. The final version may differ from this version.

This figure provides quantitative evidence that the subcellular repartition of MTX is cell line dependent.

The relative fraction of MTX bound to DNA was nearly similar in both cell lines (≈ 50% of the overall intracellular drug fluorescence). Quantitatively, the maximum fluorescence level (MTX-DNA) was nearly 2-fold higher in MCF-7 than in MDA-MB-231. In both cell lines, DHA supplementation did not change significantly the relative contribution of the MTX-DNA complex to the intracellular drug fluorescence.

MTX level in cytosol (native plus metabolized MTX) was higher in MCF-7 (18890 ± 889 a.u.) than in MDA-MB-231 (4452 ± 603 a.u.). In contrast, proportion of the MTX-metabolite in cytosol was much higher in MDA-MB-231 (60.4 ± 6.2 %) than in MCF-7 (7.7 ± 1.9 %). After DHA supplementation, cytosolic content of MTX increased (to 10157 ± 768 a.u.) in MDA-MB-231, but not in MCF-7. Proportion of the metabolite increased up to 94.2 ± 2.6 % in MDA-MB-231 and to 31.6 ±2.3 % in MCF-7. When cells were pre-treated for 15 min with the antioxidant N-acetyl-L-cysteine (NAC), the enhancement of the metabolized MTX fraction by DHA was no longer observed. This indicates that the metabolite may be related to oxidative metabolism of the drug.

Fluorescence level of MTX in low polarity environment (membranes) was similar in both cell lines (≈ 2600 a.u.). DHA supplementation had no significant effect on the fluorescence levels observed in these compartments.

ROS levels. The ROS levels were similar in both cell lines (1689 ± 117 a.u./mg proteins in MDA-MB-231 cells and 1663 ± 95 a.u./mg proteins in MCF-7 cells). These levels were not modified neither by DHA supplementation nor MTX treatment. An 1.3-fold increase ($p < 0,001$) of the ROS level was observed with MTX treatment in DHA-supplemented MDA-MB-231 but not in MCF-7 cells.

DMD Fast Forward. Published on February 12, 2007 as DOI: 10.1124/dmd.106.013474
This article has not been copyedited and formatted. The final version may differ from this version.

DISCUSSION

The above results demonstrate for the first time an association between the chemosensitization of a breast cancer cell line and the cellular distribution and metabolism of an anticancer agent. For achieving this conclusion, we used an experimental system involving two human breast cancer cell lines with a differential sensitivity to several drugs (Mahéo et al., 2005). Cytotoxicity data indicated that, under control conditions, IC_{50} was about 10-fold higher and overall drug intracellular concentration was 2.5-fold higher in MCF-7 than in MDA-MB-231, showing that MCF-7 is less sensitive to MTX compared to MDA-MB-231. We took advantage of the differential chemosensitivity of the two breast cancer cell lines to examine the contribution of drug subcellular distribution in this phenomenon. Confocal spectral imaging provided the opportunity to address the subcellular distribution of anticancer drug according to its molecular interaction within cellular compartments.

In agreement with the main mechanism of MTX action, i.e. inhibition of nuclear enzyme topoisomerase II, the nuclear drug staining (MTX-DNA fraction) was dominant in both cell lines. However, the higher level of MTX-DNA complexes in the less sensitive MCF-7 suggests that cell sensitivity to MTX is not a direct consequence of the nuclear accumulation of the drug. Indeed, the repartition and metabolism of the drug in the cytosolic compartment were significantly different between the two cell lines. The staining of the cytosolic complex of native MTX was less intense and less homogenous in MDA-MB-231 than in MCF-7. A special attention should be paid to the metabolite fluorescence, since it was particularly intense in MDA-MB-231. As indicated by the CSI maps, the metabolite was mainly concentrated in perinuclear areas rich in membranes. These areas were not assignable to mitochondria, since they were not co-localized with staining of a mitochondrial fluorescent marker, rhodamine 123. The oxidative pathway of this metabolism was indicated by its

inhibition after pre-treatment of the cells with NAC antioxydant. In view of this, the most likely assignment of the organelles responsible for MTX metabolism is endoplasmic reticulum, rich in oxidation phase I enzymes. This hypothesis was supported by co-localization of this metabolite fluorescence with emission of ER-Tracker™ Green, an endoplasmic reticulum probe.

The observation that MDA-MB-231, and not MCF-7, is chemosensitizable by DHA, a peroxidizable polyunsaturated fatty acid, provided the opportunity to examine the involvement of MTX localization or metabolism in chemosensitivity. DHA enhanced the sensitivity of MDA-MB-231 to MTX, while it had no effect on MCF-7. CSI data showed that DHA increased MTX accumulation in MDA-MB-231, and not in MCF-7. This accumulation occurred in cytosol, and was assigned to metabolized MTX, suggesting a role for this metabolism in DHA-enhanced MTX activity.

Reska et al. indicated that MTX and related molecules are easily subject to oxidative enzymatic action (Reszka et al., 1986). Enzymatic oxidation of MTX by peroxidase in presence of hydrogen peroxide led to a cyclic metabolite (Kolodziejczyk et al., 1988; Bruck and Harvey, 2003). In our study, the observed metabolite had a fluorescence emission maximum at 654 nm, similarly to the one described by Feofanov et al (Feofanov et al., 1997a) and supposed by these authors to be a cyclic metabolite. However, the fluorescence spectrum does not provide sufficient structural specificity to assign the emission to an exact chemical formula. Identification of the exact metabolite structure should be a subject of further studies implying structurally-specific analytical techniques like vibrational spectroscopy, NMR and mass spectrometry. Therefore we conclude that the metabolite detected in the present study was a fluorescent molecule originated from MTX oxidation within cancer cells. Isolation of metabolite and identification of its structure would allow evaluating its direct cytotoxicity.

Brück and Harvey (Bruck and Harvey, 2003) have reported that highly oxidized MTX metabolites form covalent complexes with DNA and inhibit DNA replication enzymes and may contribute to the cytotoxic effects of the drug (Panousis et al., 1995; Panousis et al., 1997). However, we can note that in our conditions there was no detectable staining of metabolite in nucleus. In alternative to direct nuclear action of the metabolite, we hypothesize that it could contribute to chemosensitivity by influencing cell oxidative status. Indeed, it was shown that the peroxidative conversion of MTX is accompanied by formation of free radical species (Kolodziejczyk et al., 1988). However, in the present study, MTX treatment of both cell lines did not lead to an increase of ROS as measured with CM-H_2DCFDA. In contrast, ROS levels were increased by MTX in DHA-supplemented MDA-MB-231 cells.

The polyunsaturated fatty acid DHA, with its 6 double-bonds, is very prone to oxidation and therefore provides abundant targets for ROS. We previously demonstrated that DHA supplementation leads to a high lipid peroxidation in MDA-MB-231, and to a moderate lipid peroxidation in MCF-7 cells (Maheo et al., 2005). This is in accordance with our current observation of a high concentration of an oxidized MTX metabolite in MDA-MB-231 cells and a low concentration of the metabolite in MCF-7 cells. Products of lipid peroxidation such as hydroperoxides and aldehydes have been implicated in cytotoxic process and increase drug efficacy (Das, 2002; Stoll, 2002; Dianzani, 2003). This might explain why NAC inhibited the DHA-induced enhancement of MTX toxicity in MDA-MB-231 cells. Thus, conditions favoring an increased lipid peroxidation in response to MTX would lead to a higher activity of the drug. Further studies of enzymes responsible for MTX metabolism should bring complementary knowledge on different sensitivity of cancer cell lines to antitumor agents, necessary to explore new therapeutic perspectives.

REFERENCES

Bell DH (1988) Characterization of the fluorescence of the antitumor agent, mitoxantrone. *Biochim Biophys Acta* 949:132-137.

Bruck TB and Harvey PJ (2003) Oxidation of mitoxantrone by lactoperoxidase. *Biochim Biophys Acta* 1649:154-163.

Burns CP, Haugstad BN, Mossman CJ, North JA and Ingraham LM (1988a) Membrane lipid alteration: effect on cellular uptake of mitoxantrone. *Lipids* 23:393-397.

Burns CP and North JA (1986) Adriamycin transport and sensitivity in fatty acid-modified leukemia cells. *Biochim Biophys Acta* 888:10-17.

Burns CP, North JA, Petersen ES and Ingraham LM (1988b) Subcellular distribution of doxorubicin: comparison of fatty acid-modified and unmodified cells. *Proc Soc Exp Biol Med* 188:455-460.

Colas S, Germain E, Arab K, Maheo K, Goupille C and Bougnoux P (2005) Alpha-tocopherol suppresses mammary tumor sensitivity to anthracyclines in fish oil-fed rats. *Nutr Cancer* 51:178-183.

Colas S, Paon L, Denis F, Prat M, Louisot P, Hoinard C, Le Floch O, Ogilvie G and Bougnoux P (2004) Enhanced radiosensitivity of rat autochthonous mammary tumors by dietary docosahexaenoic acid. *Int J Cancer* 109:449-454.

Consoli U, Van NT, Neamati N, Mahadevia R, Beran M, Zhao S and Andreeff M (1997) Cellular pharmacology of mitoxantrone in p-glycoprotein-positive and -negative human myeloid leukemic cell lines. *Leukemia* 11:2066-2074.

Das U (2002) A radical approach to cancer. *Med Sci Monit* 8:RA79-92.

Das UN (1999) Essential fatty acids, lipid peroxidation and apoptosis. *Prostaglandins Leukot Essent Fatty Acids* 61:157-163.

Dianzani MU (2003) 4-hydroxynonenal from pathology to physiology. *Mol Aspects Med* 24:263-272.

Feofanov A, Charonov S, Fleury F, Kudelina I, Jardillier JC and Nabiev I (1999) Confocal spectral imaging analysis of intracellular interactions of mitoxantrone at different phases of the cell cycle. *Anticancer Res* 19:5341-5348.

Feofanov A, Sharonov S, Fleury F, Kudelina I and Nabiev I (1997a) Quantitative confocal spectral imaging analysis of mitoxantrone within living K562 cells: intracellular accumulation and distribution of monomers, aggregates, naphtoquinoxaline metabolite, and drug-target complexes. *Biophys J* 73:3328-3336.

Feofanov A, Sharonov S, Kudelina I, Fleury F and Nabiev I (1997b) Localization and molecular interactions of mitoxantrone within living K562 cells as probed by confocal spectral imaging analysis. *Biophys J* 73:3317-3327.

Fox ME and Smith PJ (1995) Subcellular localisation of the antitumour drug mitoxantrone and the induction of DNA damage in resistant and sensitive human colon carcinoma cells. *Cancer Chemother Pharmacol* 35:403-410.

Germain E, Chajes V, Cognault S, Lhuillery C and Bougnoux P (1998) Enhancement of doxorubicin cytotoxicity by polyunsaturated fatty acids in the human breast tumor cell line MDA-MB-231: relationship to lipid peroxidation. *Int J Cancer* 75:578-583.

Germain E, Lavandier F, Chajes V, Schubnel V, Bonnet P, Lhuillery C and Bougnoux P (1999) Dietary n-3 polyunsaturated fatty acids and oxidants increase rat mammary tumor sensitivity to epirubicin without change in cardiac toxicity. *Lipids* 34 Suppl:S203.

Gewirtz DA (1999) A critical evaluation of the mechanisms of action proposed for the antitumor effects of the anthracycline antibiotics adriamycin and daunorubicin. *Biochem Pharmacol* 57:727-741.

Hazlehurst LA, Foley NE, Gleason-Guzman MC, Hacker MP, Cress AE, Greenberger LW, De Jong MC and Dalton WS (1999) Multiple mechanisms confer drug resistance to mitoxantrone in the human 8226 myeloma cell line. *Cancer Res* 59:1021-1028.

Kellner U, Hutchinson L, Seidel A, Lage H, Danks MK, Dietel M and Kaufmann SH (1997) Decreased drug accumulation in a mitoxantrone-resistant gastric carcinoma cell line in the absence of P-glycoprotein. *Int J Cancer* 71:817-824.

Kolodziejczyk P, Reszka K and Lown JW (1988) Enzymatic oxidative activation and transformation of the antitumor agent mitoxantrone. *Free Radic Biol Med* 5:13-25.

Litman T, Brangi M, Hudson E, Fetsch P, Abati A, Ross DD, Miyake K, Resau JH and Bates SE (2000) The multidrug-resistant phenotype associated with overexpression of the new ABC half-transporter, MXR (ABCG2). *J Cell Sci* 113 (Pt 11):2011-2021.

Maheo K, Vibet S, Steghens JP, Dartigeas C, Lehman M, Bougnoux P and Gore J (2005) Differential sensitization of cancer cells to doxorubicin by DHA: A role for lipoperoxidation. *Free Radic Biol Med* 39:742-751.

Menendez JA, Lupu R and Colomer R (2005) Exogenous supplementation with omega-3 polyunsaturated fatty acid docosahexaenoic acid (DHA; 22:6n-3) synergistically enhances taxane cytotoxicity and downregulates Her-2/neu (c-erbB-2) oncogene expression in human breast cancer cells. *Eur J Cancer Prev* 14:263-270.

Menendez JA, Ropero S, Lupu R and Colomer R (2004) Omega-6 polyunsaturated fatty acid gamma-linolenic acid (18:3n-6) enhances docetaxel (Taxotere) cytotoxicity in human breast carcinoma cells: Relationship to lipid peroxidation and HER-2/neu expression. *Oncol Rep* 11:1241-1252.

Mosmann T (1983) Rapid colorimetric assay for cellular growth and survival: application to proliferation and cytotoxicity assays. *J Immunol Methods* 65:55-63.

Novak RF and Kharasch ED (1985) Mitoxantrone: propensity for free radical formation and lipid peroxidation--implications for cardiotoxicity. *Invest New Drugs* 3:95-99.

Panousis C, Kettle AJ and Phillips DR (1995) Myeloperoxidase oxidizes mitoxantrone to metabolites which bind covalently to DNA and RNA. *Anticancer Drug Des* 10:593-605.

Panousis C, Kettle AJ and Phillips DR (1997) Neutrophil-mediated activation of mitoxantrone to metabolites which form adducts with DNA. *Cancer Lett* 113:173-178.

Reszka K, Kolodziejczyk P and Lown JW (1986) Horseradish peroxidase-catalyzed oxidation of mitoxantrone: spectrophotometric and electron paramagnetic resonance studies. *J Free Radic Biol Med* 2:25-32.

Rose DP and Connolly JM (1999) Omega-3 fatty acids as cancer chemopreventive agents. *Pharmacol Ther* 83:217-244.

Shao Y, Pardini L and Pardini RS (1995) Dietary menhaden oil enhances mitomycin C antitumor activity toward human mammary carcinoma MX-1. *Lipids* 30:1035-1045.

Sharonov S, Chourpa I, Morjani H, Nabiev I, Manfait M and Feofanov A (1994) Confocal spectral imaging analysis in studies of the spatial distribution of antitumour drugs within living cancer cells. *Analytica Chimica Acta* 290:40-47.

Smith PJ, Desnoyers R, Blunt N, Giles Y, Patterson LH and Watson JV (1997) Flow cytometric analysis and confocal imaging of anticancer alkylaminoanthraquinones and their N-oxides in intact human cells using 647-nm krypton laser excitation. *Cytometry* 27:43-53.

Smith PJ, Sykes HR, Fox ME and Furlong IJ (1992) Subcellular distribution of the anticancer drug mitoxantrone in human and drug-resistant murine cells analyzed by flow cytometry and confocal microscopy and its relationship to the induction of DNA damage. *Cancer Res* 52:4000-4008.

Spector AA and Burns CP (1987) Biological and therapeutic potential of membrane lipid modification in tumors. *Cancer Res* 47:4529-4537.

Stoll BA (2002) N-3 fatty acids and lipid peroxidation in breast cancer inhibition. *Br J Nutr* 87:193-198.

FOOTNOTES

a) Unnumbered footnote

This work was supported in part by grants from Ligue Nationale contre le Cancer (Comités d'Indre et Loire, Loir et Cher, Indre), by Institut National de la Santé et de la Recherche Médicale (INSERM: Action Thématique Concertée "Nutrition"), by Conseil Régional (Région Centre) and by Cancéropôle Grand-Ouest. Sophie Vibet was the recipient of a fellowship from the Ministère de l'Enseignement Supérieur et de la Recherche.

b) Person to receive reprint requests

Professor Igor CHOURPA

Faculté de Pharmacie,

31 avenue Monge

37100 Tours, France.

e-mail : chourpa@univ-tours.fr

DMD Fast Forward. Published on February 12, 2007 as DOI: 10.1124/dmd.106.013474
This article has not been copyedited and formatted. The final version may differ from this version.

LEGENDS FOR FIGURES

Figure 1. Reference fluorescence spectra of intracellular MTX (chemical formula in the insert): MTX-DNA complex (a), cytosolic complex of native MTX (b), cytosolic complex of metabolized MTX (c) and MTX in low polarity environment (d).

Figure 2. Dose-response curve of MTX in the absence (■) or in the presence (▲) of DHA 30 µM. Breast cancer cell lines (MDA-MB-231 and MCF-7) were grown for 7 days with specified concentration of MTX (in µM) without or with DHA 30 µM. Cell viability was measured by MTT method (see Materials and Methods). Shown are fitted curves and means ± SE from 6 separate experiments in which triplicate measurements were made. Absent error bars indicate that errors fell within symbol.

Figure 3. Typical maps of relative subcellular distribution of MTX in MCF-7 (left panel) or MDA-MB-231 (right panel). Cells were supplemented or not with 30 µM DHA for 7 days, then incubated with 0.5 µM of MTX for 1 hour. A: subcellular distribution of MTX species. The relative intensity scale of the maps (heat-intensity color code) was obtained by normalizing on the most intense spectrum in each cell. B: superposition of the maps using extended intensity scale for co-localization and encoded with pseudo-colors.

Figure 4. Co-localization of the oxidative MTX metabolite with endoplasmic reticulum within MDA-MB-231 cells (n=10). A: the fluorescence spectrum from cytosol (black curve) contains the green emission of ER-Tracker™ Green together with the red emission of the MTX metabolite. B-D: video capture of a cell (B) merged with fluorescence of ER-Tracker™ Green (C) and of MTX oxidative metabolite (D).

Figure 5. Average fluorescence levels in arbitrary units of the four species of MTX, in the two breast cancer cell lines supplemented for 7 days without (white bar) or with DHA 30 μM (grey bar). MTX-metabolite was indicated with stripes. Data are means ± SD of 16 to 23 cells.

DMD Fast Forward. Published on February 12, 2007 as DOI: 10.1124/dmd.106.013474
This article has not been copyedited and formatted. The final version may differ from this version.

Table 1. Fluorescence levels (a.u.) of intracellular mitoxantrone (MTX) in the two breast cancer cell lines. Cells were treated or not with DHA 30 µM during 7 days, then incubated during 1 hour with MTX (0.5 µM). Data are mean ± SD of 16 to 23 values. Unpaired *t*-test (not significant: $^{ns}p > 0.05$, significant: $^{***}p < 0.001$).

	MCF-7	**MDA-MB-231**
Control	38 974 ± 6 276	15 827 ± 1 746
DHA	38 833 ± 4 418 ^{ns}	23 567 ± 3 627 ***

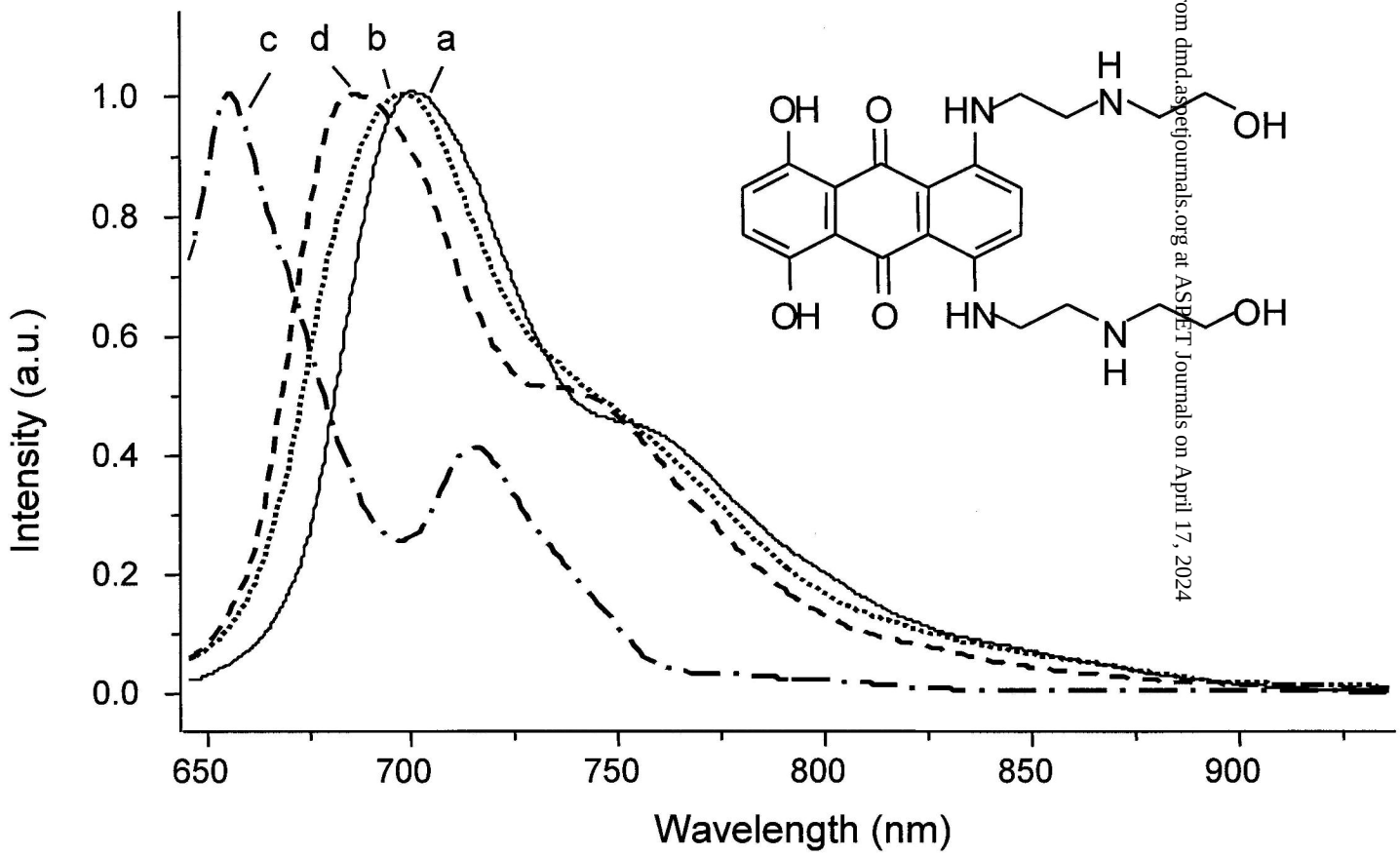

Figure 1

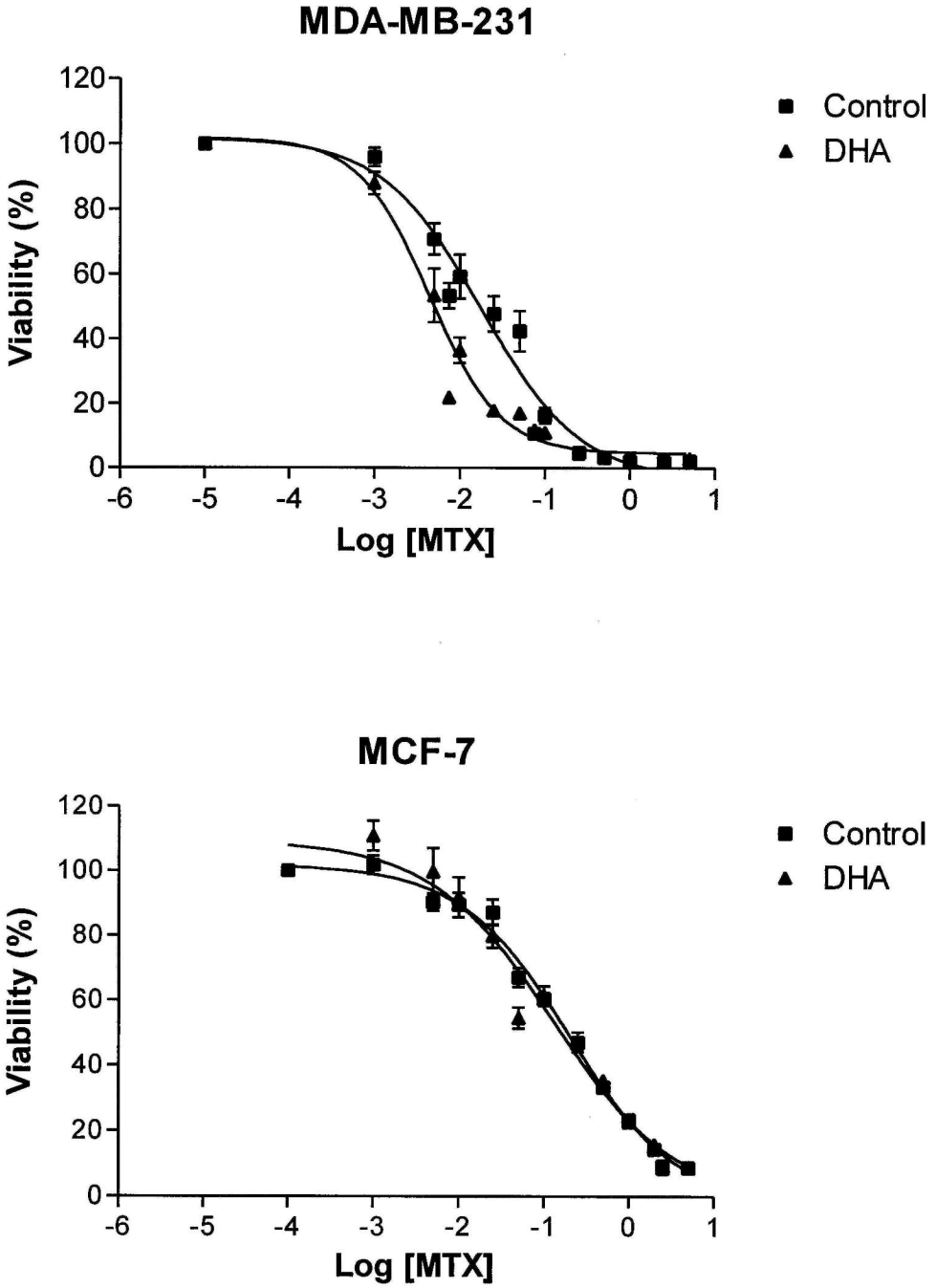

Figure 2

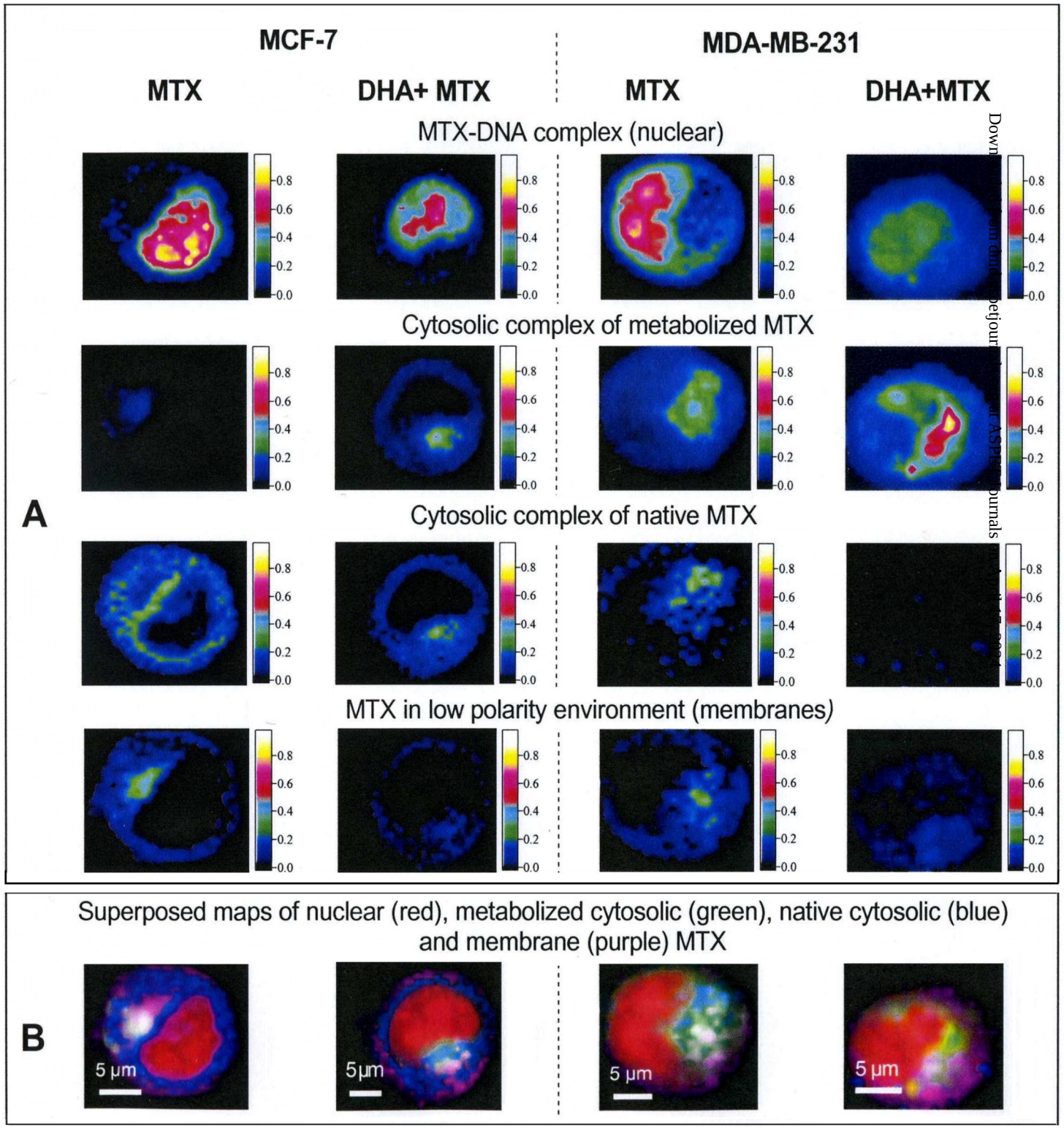
MCF-7
MDA-MB-231
MTX
DHA+ MTX
MTX
DHA+MTX
MTX-DNA complex (nuclear)
Cytosolic complex of metabolized MTX
Cytosolic complex of native MTX
MTX in low polarity environment (membranes)
A
0.8
0.6
0.4
0.2
0.0
Superposed maps of nuclear (red), metabolized cytosolic (green), native cytosolic (blue) and membrane (purple) MTX
B
5 µm

Figure 3

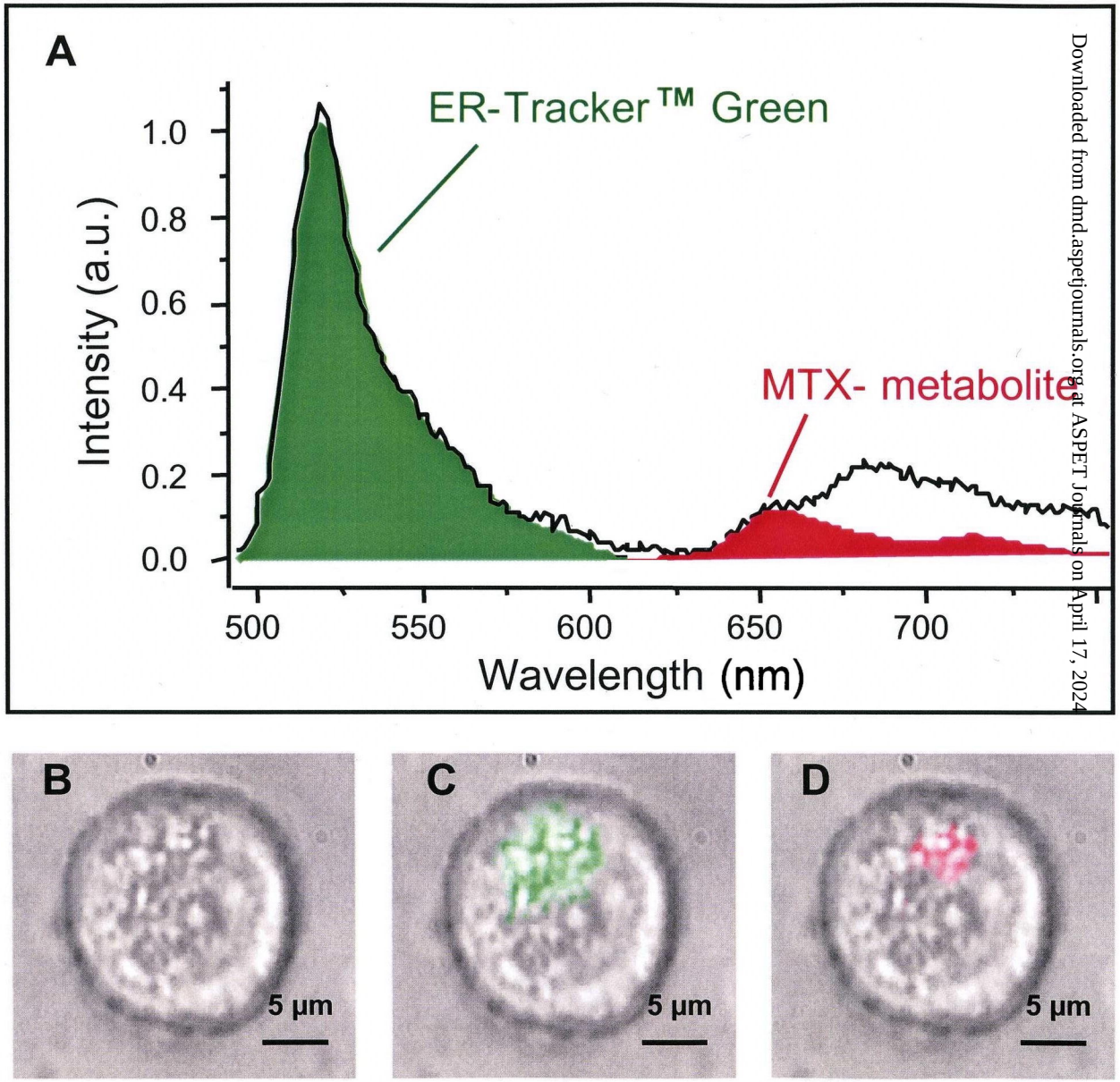

Figure 4

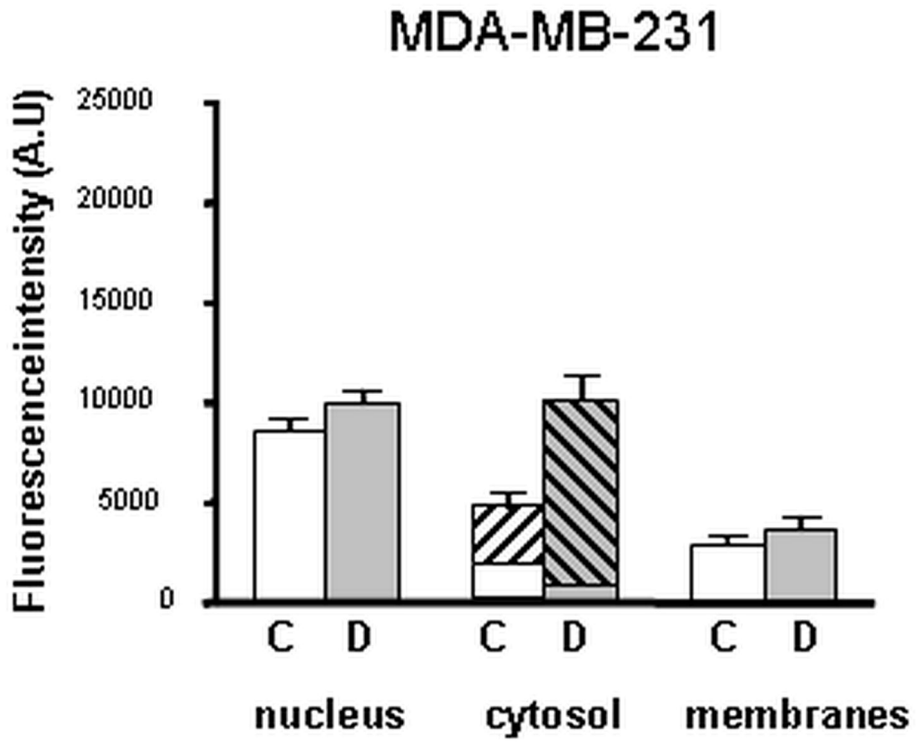

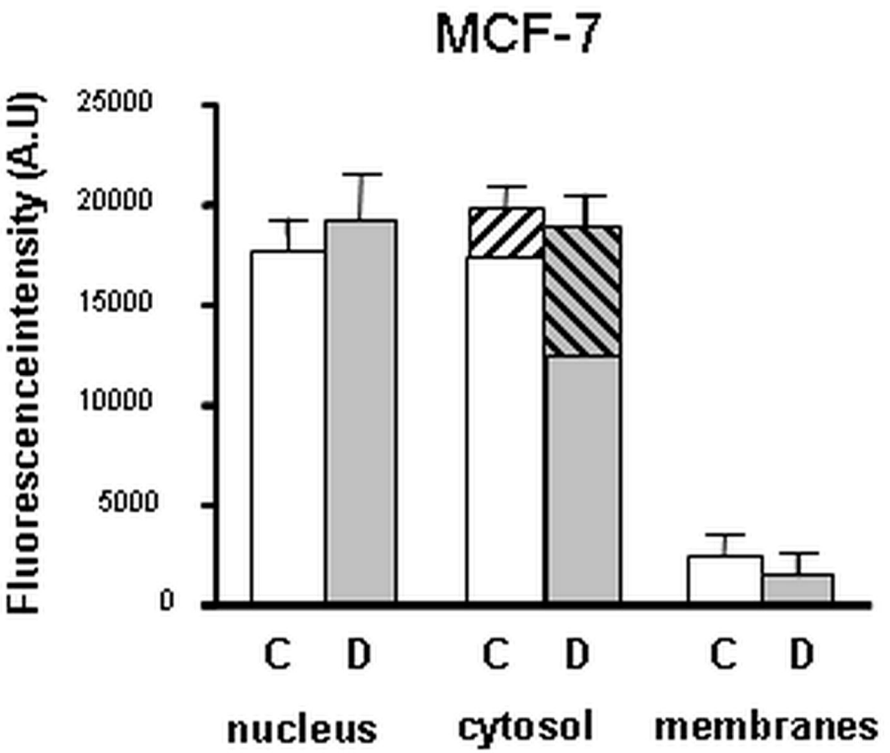

Figure 5